A MODELLING RECONSTRUCTION OF THE LAST GLACIAL MAXIMUN ICE SHEET AND ITS DEGLACIATION IN THE VICINITY OF THE NORTHERN PATAGONIAN ICEFIELD, SOUTH AMERICA

EN: GEOGRAFISKA ANNALER, N° 87 A.

REALIZADO POR:

ALUN HUBBARD
ANDREW S. HEIN
MICHAEL R. KAPLAN
NICK R.J. HULTON
NEIL GLASSER

2005

A MODELLING RECONSTRUCTION OF THE LAST GLACIAL MAXIMUM ICE SHEET AND ITS DEGLACIATION IN THE VICINITY OF THE NORTHERN PATAGONIAN ICEFIELD, SOUTH AMERICA

BY
ALUN HUBBARD[1], ANDREW S. HEIN[1], MICHAEL R. KAPLAN[1], NICK R.J. HULTON[1] AND NEIL GLASSER[2]

[1]School of GeoSciences, University of Edinburgh, Edinburgh, UK
[2]Centre for Glaciology, Institute of Geography and Earth Sciences, University of Wales, Aberystwyth, UK

Hubbard, A., Hein, A.S., Kaplan, M.R., Hulton, N.R.J. and Glasser, N., 2005: A modelling reconstruction of the late glacial maximum ice sheet and its deglaciation in the vicinity of the Northern Patagonian Icefield, South America *Geogr. Ann.*, 87 A (2): 375–391.

ABSTRACT. A time-dependent model is used to investigate the interaction between climate, extent and fluctuations of Patagonian ice sheet between 45° and 48°S during the last glacial maximum (LGM) and its subsequent deglaciation. The model is applied at 2 km resolution and enables ice thickness, lithospheric response and ice deformation and sliding to interact freely and is perturbed from present day by relative changes in sea level and equilibrium line altitude (ELA). Experiments implemented to identify an LGM configuration compatible with the available empirical record, indicate that a stepped ELA lowering of 750 to 950 m is required over 15 000 years to bracket the Fenix I–V suite of moraines at Lago Buenos Aires. However, 900 m of ELA lowering yields an ice sheet which best matches the Fenix V moraine (*c.* 23 000 a BP) and Caldenius' reconstructed LGM limit for the entire modelled area. This optimum LGM experiment yields a highly dynamic, low aspect ice sheet, with a mean ice thickness of *c.* 1130 m drained by numerous large ice streams to the western, seaward margin and two large, fast-flowing outlet lobes to the east. Forcing this scenario into deglaciation using a re-scaled Vostok ice core record results in an ice sheet that slowly shrinks by 25% to *c.* 14 500 a BP, after which it experiences a rapid collapse, loosing some 85% of its volume in *c.* 800 years. Its margins stabilize during the Antarctic Cold Reversal after which it shrinks to near present-day limits by 11 000 a BP.

Introduction

The aim of this paper is to use modelling to investigate the extent, form and fluctuations of the Northern Patagonian ice sheet from the **last glacial maximum (LGM)** through the vicissitudes of deglaciation into the early Holocene when climatic conditions were roughly analogous to those of today. Records of the LGM (Marine Isotope Stage 2) are useful because they provide a proxy for an extreme climate state, fundamentally different from the present. In particular, the glacial geologic record provides an indirect archive of former snowlines and **equilibrium line altitudes (ELAs)** during the ice age, which mirrors temperature reduction and precipitation change. In turn, numerical models can quantitatively translate the spatial and temporal record of former glacial extent into former palaeoclimatic conditions. In this particular study, we take advantage of an area where the glacial geologic record is well preserved and dated, to reconstruct palaeoglaciologic and palaeoclimatic conditions in mid-latitude South America during the LGM.

The study area

The focus of this study is a 500 × 310 km area (68 –77°W, 45–48°S) centred upon the **Northern Patagonian Icefield** (NPI) and which extends from the open Pacific Ocean in the west to the semi-arid Patagonia pampas in the east incorporating the large, cross-border lakes of Lago Buenos Aires and Lago Pueyrredon (Fig. 1a and b). The NPI is presently around 4200 km^2 and is sustained at such a low latitude by extreme precipitation rates (2–11 m a−1 w.e.) as the Southern Westerlies are forced over the Andes (Casassa *et al.* 2002). The persistence of the NPI at the very limit of Southern Hemisphere

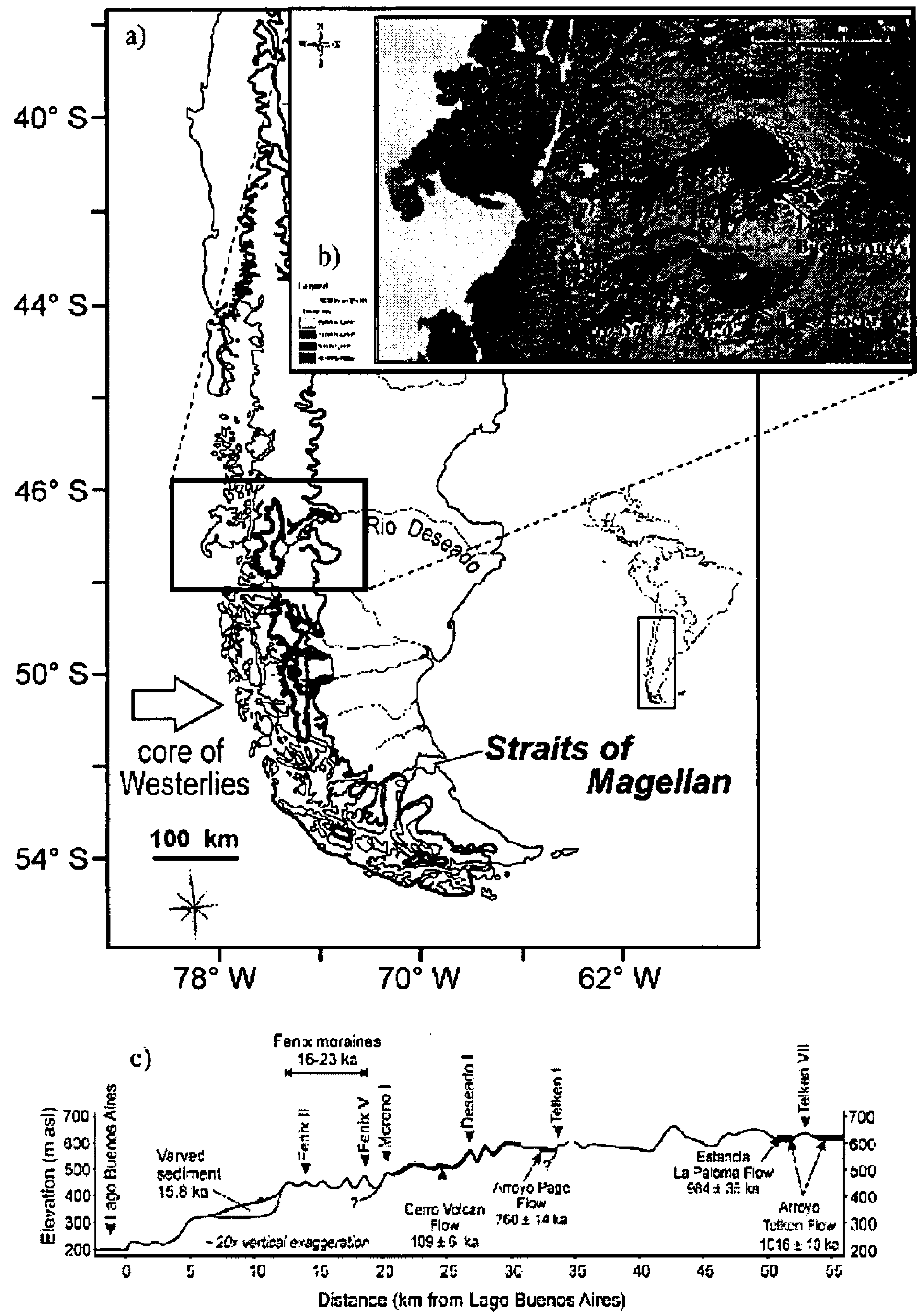

Fig. 1.(a) Map of southern Andes. (b) digital elevation model of the study area. The image shows the location of the North Patagonian Icefield (NPI) and Lago Buenos Aires (LBA) with the chronologically constrained moraine record to its east. (c) Cross-section of the moraine record east of LBA (after Kaplan *et al.* 2004)

glacierization (at 46°S, the San Rafael glacier is the lowest latitude glacier extending to sea-level on the planet) coupled with the extreme climatic gradient across the icefield, renders it highly sensitive and responsive to climate change (Kerr and Sugden 1994; Rignot *et al.* 2003). This sensitivity, coupled with the excellent geomorphic record of past fluctuations of the NPI's eastern outlet lobes, means that the area is ideally located to address some of the significant outstanding issues centred on the past latitudinal migration of the moisture-bearing westerlies and the forcing mechanisms behind regional climate and inter-hemispheric climatic synchronicity.

The geochronologic record

The LGM moraines in Patagonia were mapped by Caldenius (1932) and it is a tribute to the detail and excellence of his work that recent and considerably more intensive research efforts have led only to changes to his chronology of the depositional sequence. The moraine record at the eastern end of Lago Buenos Aires (LBA), Argentina, 46°S, is one of the oldest in the world (Rabassa and Clapperton 1990; Singer *et al.* 2004), and provides an excellent setting for numerical modelling experiments to investigate probable palaeoclimatic solutions that underpin former ice extent. Located at the middle latitudes in southern South America, the moraine record documents former glacial and climate changes and can be used to test theories of ice age climate. Most pertinent to the modelling approach, the region from LBA to the present NPI has been the focus of a major geochronologic campaign (Singer *et al.* 2004; Kaplan *et al.* 2004, 2005; Turner *et al.* 2005).

Singer *et al.* (2004) described the entire record on the eastern edge of Lago Buenos Aires in detail and presented $^{40}Ar/^{39}Ar$ ages of the lava flows that provide chronologic control for the 1 Ma glacial sequence (Fig. 1b, c). The moraines have been informally grouped into four complexes, named Fenix, Moreno, Deseado, and Telken. The oldest glacial deposit at LBA, Telken VII, is the equivalent of the **greatest Patagonian glaciation (GPG)** (Mercer 1983), and is constrained in age to *c.* 1.1 Ma. The Telken VII–I moraines were deposited between 1.016 Ma and 760 000 a BP, and the Deseado and Moreno moraines between 760 000 and 140 000 a BP (Singer *et al.* 2004). At least two Moreno moraines date to *c.* 150 000–140 000 a BP (Kaplan *et al.* 2005).

The youngest moraine set, the Fenix system, was deposited during the LGM or Marine Isotope Stage 2. Particularly relevant for this study, the Fenix moraines have been constrained in age with surface exposure and ^{14}C ages (Fig. 1c). Fenix V is *c.* 23 000 years old and represents the maximum ice extent during the last glacial maximum, and its position is a focus for the effort presented here. The youngest dated moraine, Fenix I, is *c.* 16 000 years old. Subsequently, a lake formed and then a readvance deposited the Menucos moraine (Singer *et al.* 2004). Systematic errors for the cosmogenic ages are inferred to be less than 10% (e.g. Kaplan *et al.* 2004). However, we emphasize that future systematic change in the isotopic-based ages will not affect the main results here, which are based on modelled years. Lateral moraines wrapping around the north side of Lago Buenos Aires provide a constraint on the northward extent and surface elevation of ice as it emanated from the trunk valley (Fig. 1b). On the south side, the lateral moraines end at the Meseta Lago Buenos Aires near the eastern edge of the lake. There is no evidence that ice was on top of the Meseta de Lago Buenos Aires during 'Fenix time' which is an important constraint for the our modelling effort. In addition, there is no evidence that any significant ice accumulation occurred on top of the Meseta during the last glacial maximum, except perhaps in the southwestern area (Caldenius 1932).

Whilst there is a geochronological record pinning down the timing and changing ice extent during the LGM and earlier, there is also indirect chronological control constraining the exact form and timing of the deglaciation sequence. Turner *et al.* (2005) use age constraints for onset and end of lake deposition and the timing of the rapid switch of the eastward diversion of waters draining LBA to the present westward course down the Rio Baker into the Pacific at *c.* 12 800 a BP to constrain the final separation of the North and South Patagonian Icefields. Dated shorelines created by the ice-dammed lake indicate that after 16 000 a BP, when subsequent to formation of Fenix I, eastern flowing ice lobes underwent rapid retreat to positions within 20 km of the present NPI margins. There followed a phase of relative stability starting *c.* 13 600 a BP, which was promptly terminated when the lake catastrophically drained at *c.* 12 800 a BP, potentially releasing some *c.* 2000 km^3 of fresh water into the Pacific.

Modelling strategy

Here, a three-dimensional ice flow model is used to provide an experimental framework by which the interactions between climate and ice dynamics can be investigated, validated and refined against the observed empirical record. Such modelling provides the classic link between form (the observed erosional and depositional record) and process (climate forcing and ice dynamics). The work is intended to build on and extend the modelling work of Hulton *et al.* (1994, 2002) who used a time-dependent model to investigate the extent and climate necessary to reproduce a Patagonian ice sheet that best fitted the LGM reconstruction of Holling and Schilling (1981), Porter (1981) and McCulloch *et al.* (2000). Although the ice flow model used by Hulton *et al.* (1994, 2002) captures the broad features of the LGM across South America nicely, one particular criticism that has been forcefully expressed (e.g. Lliboutry 1998; Wenzens 2003) is that the operating resolution of 10 km fails to adequately encompass the highly variable relief that characterizes the Patagonian Andes. Such a shortcoming has significant implications not only for the temporal and spatial patterns of ice flow and build-up, but also in terms of the climate forcing feedbacks driving the model.

As a consequence, Hulton *et al.* (1994, 2002) failed to replicate the large outlet lobes on the east side of the NPI which drain into Lago Buenos Aires and Lago Cochrane, even though these valleys are well over 50 km wide in places. In both LGM simulations, the 10 km flow model completely fails to adequately represent the dynamics and form of the former NPI and its outlet lobes, resulting in a large, amorphous icecap with a surface elevation of over 4500 m (which by inference results in ice thicknesses well in excess of this) completely swamping all relief (e.g. Cerro San Valentin, the highest Patagonian peak at 4056 m) and which over-runs the observed Fenix LGM limits in the east by up to 150 km.

Marshall and Clarke (1999) comprehensively discuss the resolution limitations of present ice sheet models, in particular their inability to capture alpine terrain and thus represent the processes that govern initial ice sheet conception. They present a novel, sub-grid parameterization of snow and ice distribution based on classifying mountain relief through hypsometric curves which provides a better representation of icecap inception and improves model efficacy in mountainous regions. However, even this improved topographic and mass balance representation does not alleviate a critical problem in maritime regions with extreme relief where ice masses, characterized by high accumulation rates and mass-turnover, are effectively drained and most crucially, drawn down by major ice-streams and fast-flowing outlet lobes. This is particularly the case over the Patagonian Andes and especially across the present-day icefields which experience some of the highest precipitation rates on the planet, up to 11 m a^{-1} w.e., and which have extreme topographic gradients, for example, encompassing Cerro San Valentin (4058 m) which is located within 20 km of sea-level.

In an attempt to address these issues, here an ice-flow model is applied at significantly finer resolution which we hope will provide a more sympathetic comparison with the observed geomorphic record. Specifically, the time-dependent, three-dimensional model is identical to that used by Hubbard (1999) to model the build-up and maximum extent of the Younger Dryas icecap across Scotland and has also been successfully used to investigate the LGM and subsequent deglaciation of Iceland (Hubbard *et al.* in press). It is applied to a 2 km finite-difference grid and enables the variables of ice thickness, isostatic bed adjustment and ice flow to interact freely and caters for the dynamics of ice-shelves, calving and basal sliding through longitudinal stress coupling. It is forced through perturbations from present in sea level and ELA and yields space–time distributions of ice thickness, isostatic response, stress, velocity, accumulation, ablation and iceberg flux. By running this model within a systematic experimental framework, we use it to investigate specifically:

1. the form, extent and climate forcing required to simulate the LGM limits as observed in the Fenix moraine set;
2. the sensitivity of the modelled LGM ice sheet to changes in key parameters, particularly those controlling the dynamics of the eastward-flowing outlet lobes;
3. the pattern and timing of deglaciation from 23 to 11 000 a BP using the Vostok palaeotemperature reconstruction.

Model boundary conditions and assumptions

In addition to numerous parameters (Table 1), the model also requires input distributions of basal topography and mass balance at the appropriate operating resolution.

The basal domain

The model uses a 2 km topographic grid derived from SRTM 90 m terrestrial and ETOPO2 marine global data sets, along with point bathymetry data derived from echo sounding measurements (Murdie *et al.* 1999). Though limited sub-glacial data do exist for the NPI indicating centreline ice thicknesses up to *c.* 500 m (e.g. Casassa (1987) for the Nef and Soler Glaciers; Hubbard (1999) for the San Rafael), for convenience the present-day ice surface of the NPI was taken as the basal topography in this study. Although a definite limitation, this assumption can be tentatively defended on the basis that within our study area the NPI currently covers an area less than 4200 km^2, under 5% of the total LGM ice sheet area of *c.* 90 000 km^2. The source digital elevation models were subsequently melded and interpolated onto an Albers equal-area conic projection at 2 km resolution (Fig. 1b).

The thermomechanical evolution of the ice sheet and its effect on internal deformation is not modelled; the ice sheet is assumed to be isothermal and bulk ice softness is controlled by a single parameter, the rate factor, *A*, and sliding is assumed to be universal. Critically, this identifies an important difference between the approach presented here and that of Hulton *et al.* (2002), who model the thermal evolution of the ice sheet and restrict basal sliding to zones at pressure melting point. This resulted in an LGM simulation in which extensive areas of the ice sheet are cold-based and non-sliding, resulting in an overall more viscous ice sheet model which fails to simulate the fast-flowing outlet lobes. We justify our isothermal assumption on the basis that there are virtually no data available to constrain Patagonian ice surface temperature patterns (or geothermal conditions) during the LGM and subsequent deglaciation. The common approach in ice-sheet modelling of perturbing a 'sea-level' temperature distribution corrected for ice surface elevation through a fixed lapse rate is extremely sensitive to the lapse rate chosen, which is not only highly variable across the Patagonian Andes, but furthermore, is virtually impossible to constrain in the past. For this same reasoning, we adopt a simplified mass-balance calculation, described below, rather than a more sophisticated degree-day or energy-balance approach which again, in this particular instance, merely adds additional complexity and parameterization without any gain in insight. Besides, it is well established (e.g. Hindmarsh 1993) and as sensitivity tests reveal, changing internal viscosity does not greatly affect overall model outcome in terms of spatial extent.

The lithospheric response time is nominally set at 2000 years, which represents a relatively soft lithosphere consistent with tectonically active mountain ranges like the New Zealand Alps (Paterson 1994; Van der Veen 1999). A Weertman-type sliding relation is applied and controlled by the sliding parameter, A_S, and its specific implementation is described by Hubbard (1999).

Table 1. Model Parameters

Model Parameter	Units	Accepted Range	Best-Fit LGM
Mx marine	m a^{-1}	2–6	4
Zx marine	M	900–1500	1200
Mx continental	m a^{-1}	0.1–0.4	0.25
Zx continental	m	200–600	425
Mar-Stop	km	160–190	175
Cont-Start	km	255–320	285
Weertman, *As*	Pa^{-3} s^{-1}	50×10^{-15}–100×10^{-15}	75×10^{-15}
Rate Factor, *A*	Bar^{-3} a^{-1}	0.215–0.0155	0.1
Calving, *Ac*	m a^{-1}	0.2–0.6	0.3

The surface mass balance

The model is coupled to climate by means of simplified climate parameterization where the net mass-balance is dependent on elevation and varies parabolically about the ELA in the manner used by Hulton *et al.* (1994). In this approach, two parameters control the specific shape of the parabolic curve, Mx, the maximum mass-balance and Zx, the vertical distance above ELA at which Mx is reached (Fig. 2a) so that a broad spectrum of mass-balance/elevation relationships can be defined. The extreme climatic gradient across the southern Andes is accommodated by allowing the specification of two contrasting mass-balance regimes, maritime and continental, each determined through their specific Mx and Zx parameters. The east to west graduation between these regimes is specified through the distance in an easterly direction at which full marine conditions end (mar_stop), and at which full continental conditions begin (con_start), with a linear function controlling the transition between these two (Table 1).

This mass balance parameterization is then driven by wholesale raising/lowering of a pre-defined ELA surface, a method that has been used effectively in previous modelling efforts (e.g. Boulton *et al.* 2003; Hagdorn 2003; Hulton *et al.* 1994; Hulton and Sugden 1997, Hubbard 1997) and is useful when limited or absent palaeoclimatic data restrict the use of a more sophisticated treatment.

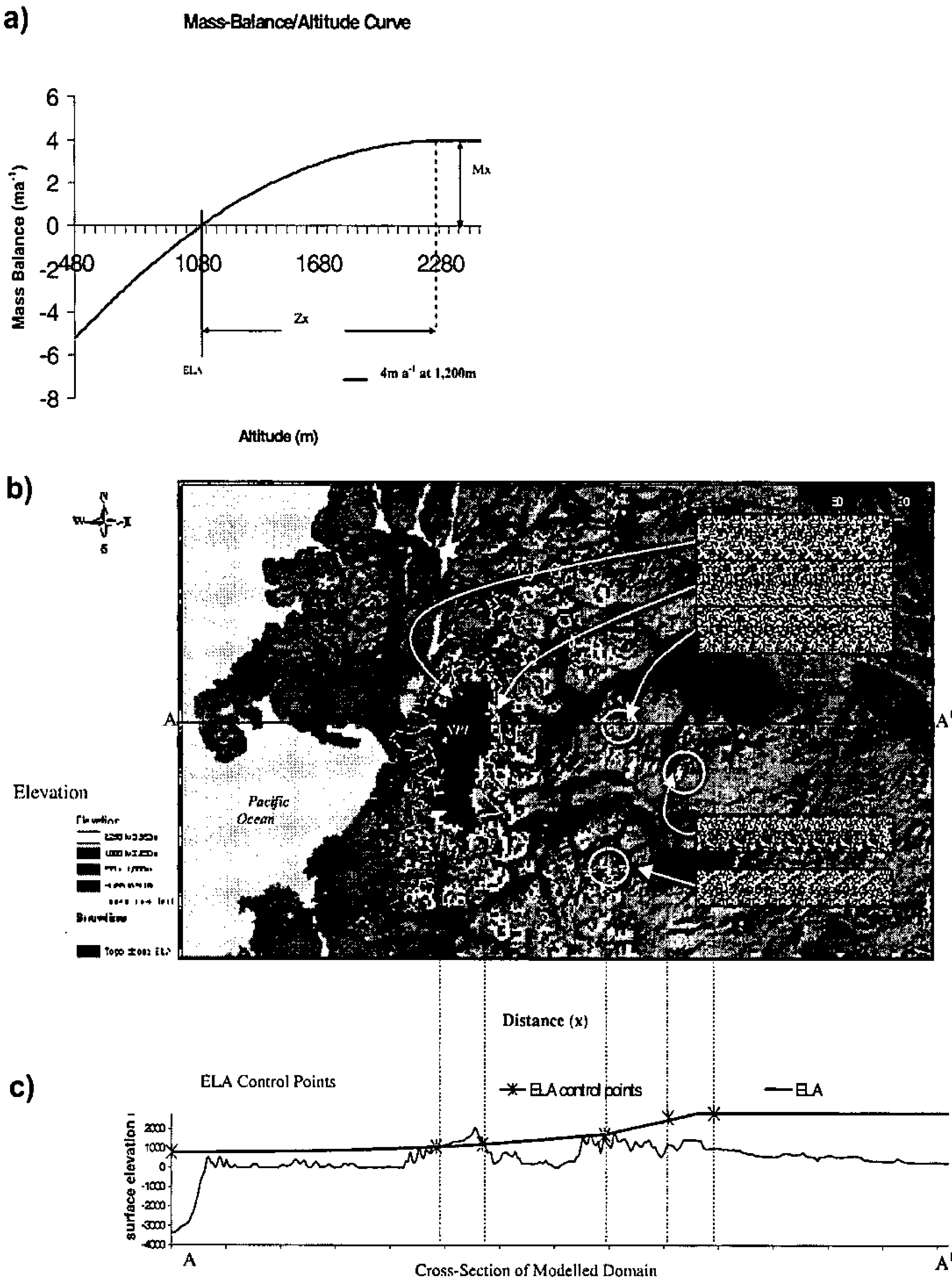

Fig. 2. a) Example of mass-balance/altitude relationship with ELA. (b) Location of control points used to define ELA surface. Topography above modelled ELA surface (black) is also shown superimposed on digitized current ice-extent (white outline). It should be noted that only major ice centres and glaciers were digitized. Many smaller satellite glaciers exist but were not digitized. (c) Cross-section of DEM showing final modern-day ELA surface with distance across entire domain. Note topography only represents line from A to A1

The ELA surface

The form of the modern-day ELA surface across the NPI which is assumed in this study to represent the general trend of that which existed in the past, varies only in the east–west direction, with no north to south variations across the 3° of latitude (Broecker and Denton 1989; Hulton *et al.* 1994). The present-day east–west ELA trend was determined by using the snowline elevation or ELA at a number of key glaciers and glacierized massifs on and around NPI (Fig. 2b; Rignot *et al.* 2003). Given that the ELA or snow-line is a continually changing surface and measured data may be influenced by recent conditions, our 'control points' were assigned a target elevation (a best estimate) and an acceptable range outside this (Fig. 2c). The trend surface was then allowed to vary within the accepted range until a best-fit was achieved using a Boltzmann sigmoidal equation:

$$ELA(x) = ((a-b)/(1 + EXP\,((distance(x)-c)/d))) + b$$

where: x is distance (in km), $a = 774$, $b = 2572$, $c = 272$ and $d = 64$.

Comparison of highland topography lying above this synthetic ELA surface (i.e. modelled accumulation areas) and current ice-extent (digitized from Landsat imagery and 1: 50 000 maps) displays a high level of correspondence (Fig. 2b). Furthermore, the 63% proportion of accumulation to total area calculated for the NPI is well within acceptable bounds of the 2:1 accumulation to ablation area ratio generally assumed for an ice mass in steady state (Paterson 1994). As explained below, the form of the ELA surface required slight modification through a linear increase on the eastern side to prevent ice build-up on the Meseta del Lago Buenos Aires during LGM. The condition of an 'ice-free' meseta is indicated by any lack of glacial geologic evidence for ice flow on or off the Meseta (Caldenius 1932; Singer *et al.* 2004), including the form of the Fenix lateral moraines and other glacial deposits, which can be traced continuously around the north side of the Meseta back to the western end of LBA.

Domain boundaries

Since the model domain occupies a somewhat arbitrary transect of the southern Andes, an artificial boundary condition must be specified when ice advances to the northern and southern limits. An assumption of constant mass flux out of the domain is made under these conditions. The east and west boundaries remain free though westward ice-extent is held in check by a calving function, related to ice thickness, front geometry, water depth and a calving parameter, Ac, in conjunction with the continental shelf which drops off to abyssal depths of over 4000 m.

Model parameters

The mass-balance parameter range is based on estimates of maximum and minimum precipitation rates for the west coast and arid interior. Prohaska (1976) presented isohyets that showed the uniformity of the precipitation gradient east of the divide which, in combination with field observations (Caldenius 1932; Kaplan *et al.* 2004; Singer *et al.* 2004), constrained continental aridity. Table 1 provides the best-fit mass balance and ice-flow parameters bracketed by acceptable limits.

The LGM simulation

To simulate the LGM ice extent, widespread virtual glaciation was introduced through a stepped lowering of ELA based on palaeoclimatic information available from a number of sources (e.g. Lamy *et al.* 2002; Becquey and Gersonde 2003; EPICA 2004). Estimates of ELA depression during the LGM range from 350 m (Hulton *et al.* 1994) to *c.* 1000 m (Broecker and Denton 1989) at 46°S. Hence, a suite of experiments was carried out, each model forced by a different ELA lowering from 400 to 1000 m in 50 m steps. Throughout all experiments, sea-level was fixed at 125 m lower than present-day in accordance with mean estimates (Fairbanks 1989). In addition, a suite of sensitivity tests was carried out by varying the mass-balance and ice-flow parameters within acceptable limits about an optimum LGM experiment. For each experiment, the model was integrated from ice-free conditions for 15 000 years until steady-state was attained and each end-member was subsequently compared against the empirical record to isolate an optimum LGM extent. This approach does introduce an important limitation in the assumption that the ice sheet and its outlet glaciers were in equilibrium with the climate responsible for them. This to some extent is acceptable insofar as we are not per se attempting to specifically reconstruct or inter-

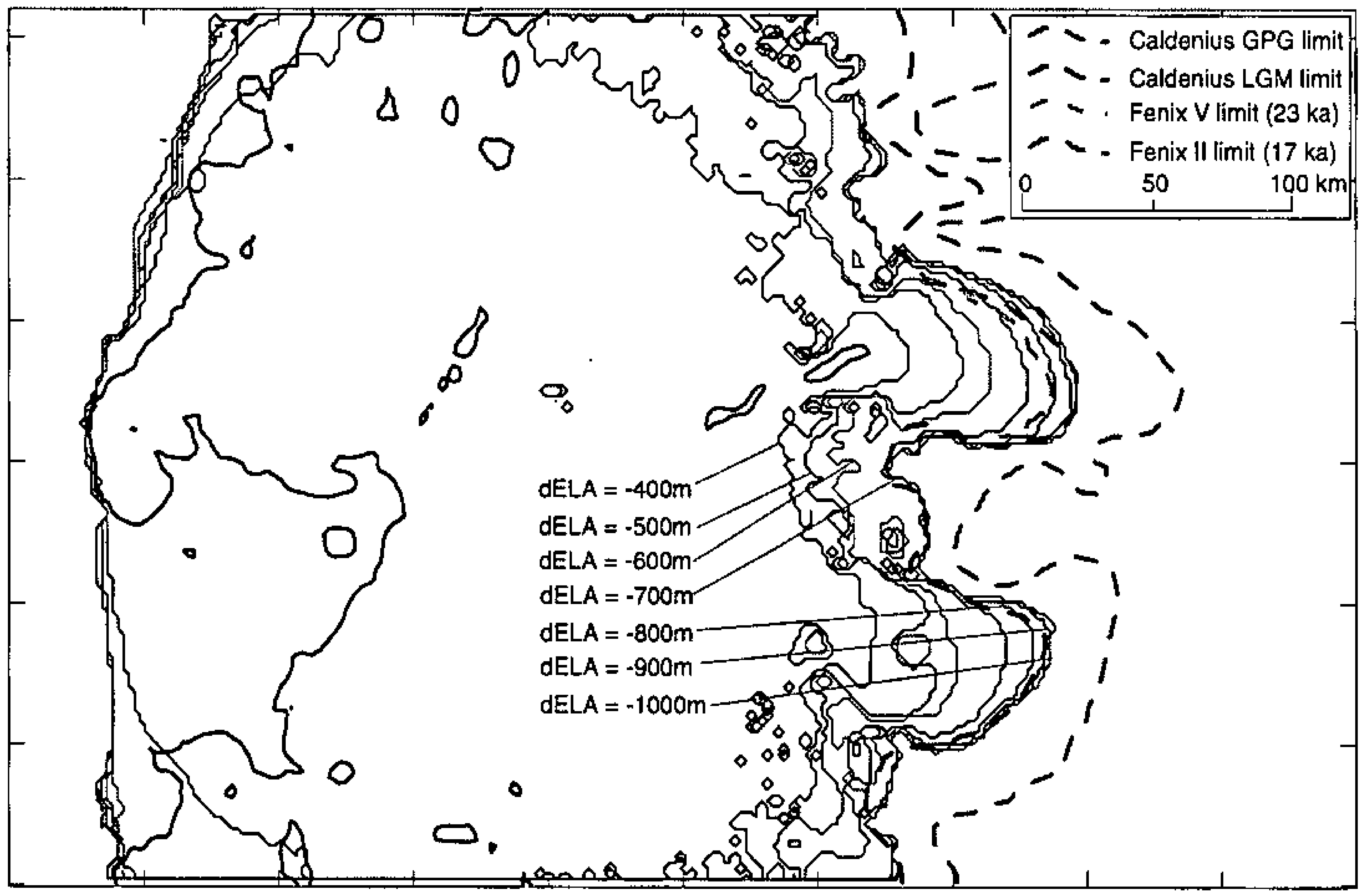

Fig. 3. Modelled ice sheet extent after 15 000 years for relative ELA forcing from 400 to 1000 m in 100 m increments

pret the LGM palaeoclimate, and as long as it is understood that our results provide a minimum estimate of the climate deterioration, then the approach is valid. In addition, that the end moraines display between 20 and 50 m of relief and are up to 500 m wide (Singer *et al.* 2004) indicates a significantly long-lived period of ice-standstill at these positions implying at least a quasi-equilibrium state which again justifies the assumption.

Comparison of steady-state LGM ice extent for different intensities of ELA forcing, illustrates the contrasting sensitivity between the east and west sides of the NPI directly reflecting the climatic regimes which dominate (Fig. 3). Whereas an ELA lowering of less than 400 m results in a series of large ice-streams out to the continental shelf edge where they calve off in rapidly deepening water, the converse is not the case, where an ELA lowering of at least 750 m is required to drive the eastward-outlet ice lobes out to the first of the Fenix moraines, demarking the LGM. Furthermore, it is apparent that these outlet lobes demonstrate a linear response, in terms of ice extent to magnitude of ELA forcing, until the Telken moraines are obtained, at which point they become practically decoupled from any additional ELA lowering (Fig. 3).

The optimum LGM model experiment which best matched the Fenix V moraine required 900 m of ELA lowering and, its terminal position is well represented (Fig. 4). Furthermore, the whole eastern margin of this **Optimum LGM Experiment (OLE)** corresponds well (within 5 km) with Caldenius' (1932) LGM limit for this sector of the Patagonian Andes from *c.* 45 to 48°S. At the western margin, active calving accounts for virtually all mass wastage and the OLE extends well offshore and to the continental slope in the central sector. Only in the far northwest and southwest, far removed from the main centres of ice accumulation, does the ice sheet not extend to the continental slope, which is most likely an artefact of the rather artificial domain boundary condition which precludes ice influx into these far-field zones.

LGM sensitivity testing

A sensitivity analysis of key model parameters was completed in order to assess the quality of the model result and how that may affect interpretation of the OLE. This was carried out by running the OLE with one parameter changed in turn, to investigate its effect on ice volume, response time and aerial

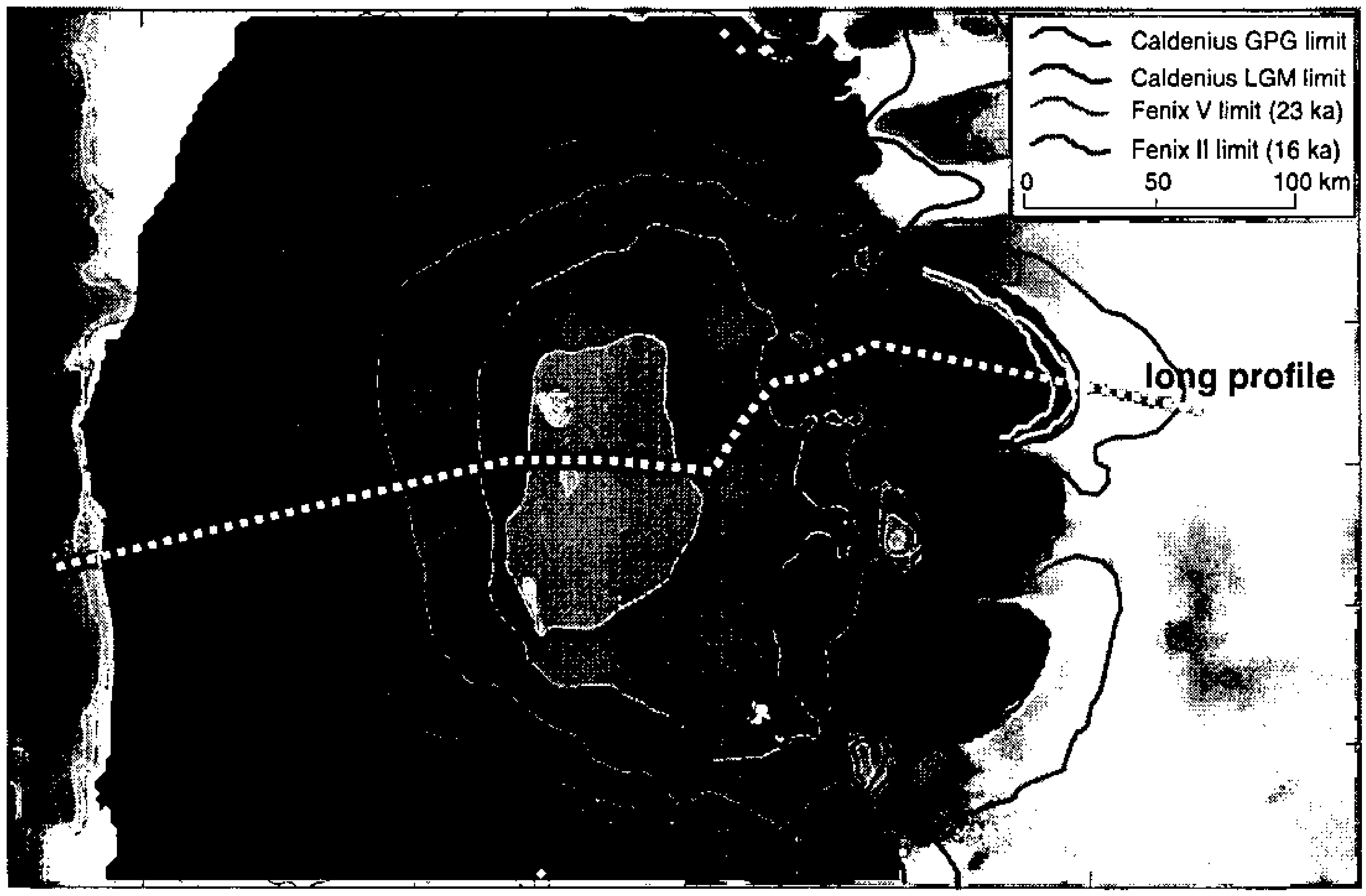

Fig. 4. Optimum LGM experiment showing the NPI modelled ice sheet extent and surface elevation after 15 000 integrated years given a stepped ELA lowering of 900 m from completely ice-free conditions. Superimposed for comparison are the Fenix II (*c.* 17 ka BP) and V (*c.* 23 ka BP) moraines along with Caldenius' (1932) LGM and Greatest Patagonian Glaciation limits. For the LBA area, Caldenius' (1932) LGM and Fenix V are considered coincident within the limits of model resolution

extent. Comparisons were then made against the OLE, which are summarized in Table 2.

The model was found to be highly sensitive to the mass-balance parameters with significant changes to ice-margin extent and overall area and volume. No surprise, given that the accepted range in the values (Table 1) result in widely different mass balance–elevation relationships (Fig. 5). Modification of the marine mass-balance regime was found to affect the entire ice sheet (Fig. 6a). The ice sheet is most sensitive to the accumulation end of the marine mass-balance curve, Mx (Fig. 5), since the ablation zone is reduced on the western side and marine accumulation also has a cross-divide effect on the eastern side. The contrary is not true though, since modifying the continental mass-balance regime primarily affects eastward extent but has little effect on the ice sheet as a whole (Fig. 6b). In particular, parameters affecting the ablation end of the curve had an extreme effect on eastward extent (Fig. 6b) since any rise in ELA consequently amplifies ablation rates (Fig. 5). The model was also sensitive to the continentality function as would be expected, since this controls transition from marine to continental conditions.

The model was not particularly sensitive to parameters affecting internal deformation and isostasy, though varying the sliding parameter had a significant effect on total ice volume but without any concomitant change in ice extent (Fig. 6c). Relaxing the calving parameter enables a faster build-up in ice volume to the west but negligible eastward advance.

The deglaciation sequence

In order to investigate the deglaciation sequence, we bump-started and forced the OLE from the Fenix V moraine using a time-series from 23 300 to 11 000 years BP based on the Vostok palaeotemperature reconstruction (Petit *et al.* 1999). This temperature record is reconstructed from the Vostok ice core deuterium record assuming a gradient of 9‰/°C after accounting for the isotopic change of sea-water. It yields a temperature series relative

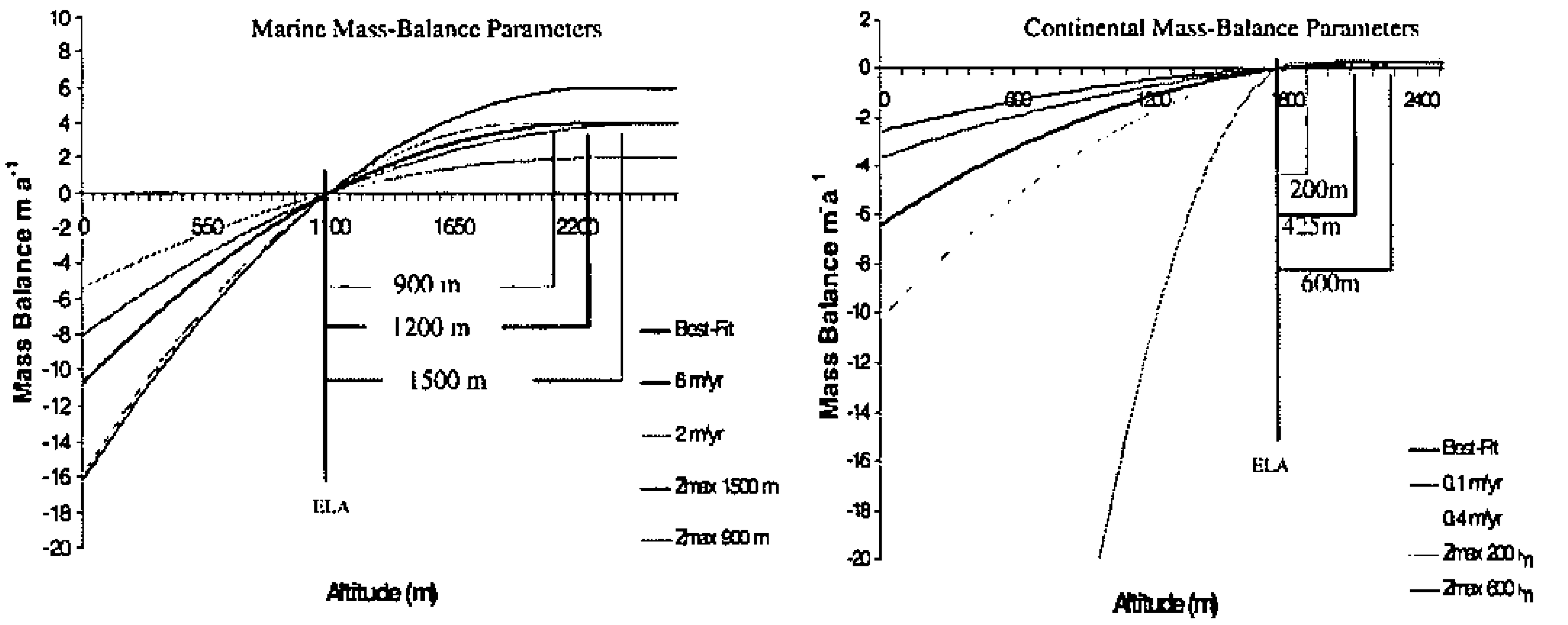

Fig. 5. The different elevation/mass-balance relationships resulting from varying the model parameters within accepted limits. Note the extreme rates of ablation potentially resulting from the continental mass-balance parameters

to the recent mean value and varies from *c.* –8.9°C at 23 300 years to *c.* 0°C at 11 000 years. For our purposes, this temperature-series was rescaled to yield a maximum ELA lowering of 900 m (the OLE condition at 23 300) to +200 m ELA at 11 000 years (Fig. 7). Although crude, such a local scaling of ELA to a far-field record does provide a low-level test of the general applicability of the Antarctic palaeoclimate record into a wider Southern Hemispheric context. It may also be justified on the basis that the Vostok deuterium excess record is itself a direct function of the meteorological and oceanic characteristics of its precipitation source regions, that is the Southern Ocean adjacent to South America (Vimeux *et al.* 2002). Furthermore, use of the Antarctic record enables us to investigate whether the timing, magnitude and span of the **Antarctic Cold Reversal (ACR)** recorded between 13 600 and 11 900 a BP in the Vostok temperature reconstruction, would have any bearing on the dynamics and response of the deglaciation sequence of the Patagonian ice mass at such a low latitude as the

Table 2. Sensitivity analysis of model parameters

Parameter	Area (km^2)	Volume (km^3)	Difference in area (%)	Difference in volume (%)	Volume variance within parameter (%)
LGM	91 872	103 247	–	–	
Mass Balance					
Mx marine 2m a^{-1}	84 704	88 204	–5.78	–17.43	
Mx marine 6m a^{-1}	94 608	121 456	5.24	13.70	37.60
Zx marine 900 m	89 628	106 718	–0.30	–0.10	
Zx marine 1500 m	89 464	105 593	–0.48	–1.15	–1.10
Mx continental 0.1 m a^{-1}	97 312	116 835	8.24	9.37	
Mx continental 0.4 m a^{-1}	87 000	102 044	–3.23	–4.48	–12.70
Zx continental 200 m	83 068	96 110	–7.60	–10.03	
Zx continental 600 m	95 036	115 129	5.71	7.77	19.80
Continental start 235 km	84 016	91 963	–6.55	–13.91	
Continental start 335 km	96 472	121 295	7.31	13.54	31.90
Ice Dynamics					
A = 0.0155 (–10°C)	89 648	106 788	–0.28	–0.04	
A = 0.215 (0°C)	89 800	105 260	–0.11	–1.47	–1.43
Isostasy = 1000 yrs	89 404	105 942	–0.55	–0.83	
Isostasy = 3000 yrs	89 016	104 625	–0.98	–2.06	–1.24
As = 50×10^{-15}	90 580	119 860	0.76	12.20	
As = 100×10^{-15}	89 048	99 322	–0.95	–7.02	–17.13

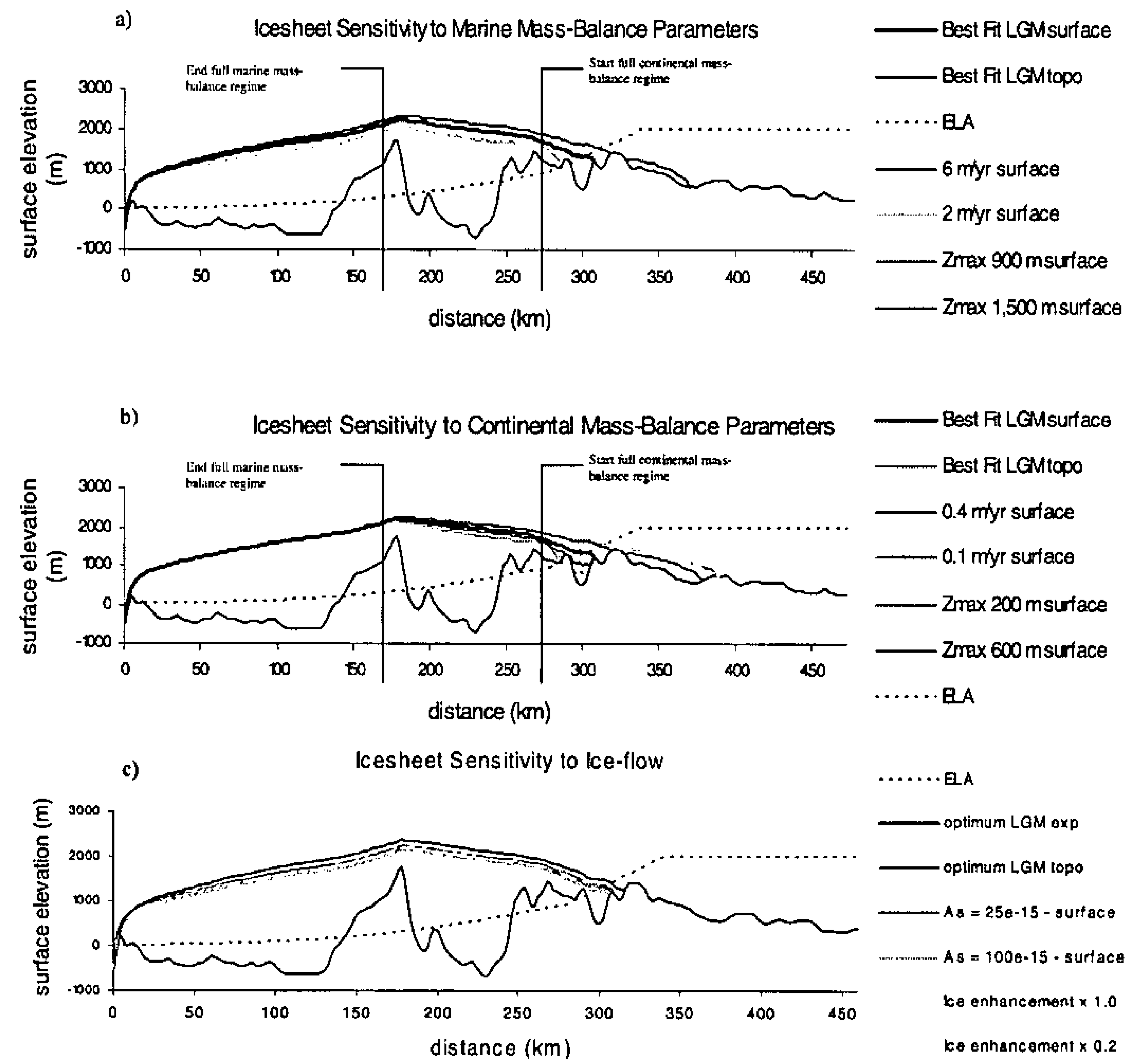

Fig. 6. Ice sheet profiles showing the effect of changing (a) marine and (b) continental mass-balance parameters, and (c) internal model parameters governing internal deformation, basal sliding, calving and isostasy. Only basal sliding (the Weertman parameter, *As*) has any appreciable effect on ice sheet form. Increasing the sliding parameter ($As = 7.5 \times 10^{-15}$) yields a lower ice sheet profile with less volume. Decreasing the sliding parameter ($As = 25 \times 10^{-15}$) raises the ice sheet profile with a corresponding increase in volume

NPI, as alluded to Turner *et al.* (2005) and Sugden *et al.* (2005).

Forcing the model from the OLE, Fenix V limit at *c.* 23 000 (Fig. 8a) through to the early Holocene at *c.* 11 000 a BP with the rescaled Vostok record results in an ice sheet that is in good agreement with the observed geochronologic record. From 23 000 to just after 17 000 a BP the ice sheet volume and area remain stable with only minor fluctuations (<2%) in ice volume and area, directly reflecting the ELA oscillations (*c.* 100 m) on a millennial time-scale driving the model. During this time, the western, seaward margin is unchanged and the two eastern outlet lobes are relatively stable with only minor advance and retreat cycles in and around their LGM positions, as indicated by the Caldenius and Fenix suite of moraines. Throughout this period the eastern lobe occupying LBA does not retreat much more than *c.* 10 km in front of the Fenix II moraine and at 17 000 a BP, following a short and final climatic dip (relative ELA to –900 m), the lobe advances to the Fenix II position (Fig. 8b).

After 17 000 years BP, reflecting a fairly steady overall rise in the ELA surface over the next *c.* 3500 years, the ice sheet undergoes, first, a phase of steady retreat reflected in relatively slow shrinkage in its western margins and eastern outlet lobes (Fig. 8c) through to *c.* 14 500 years BP when the ice sheet

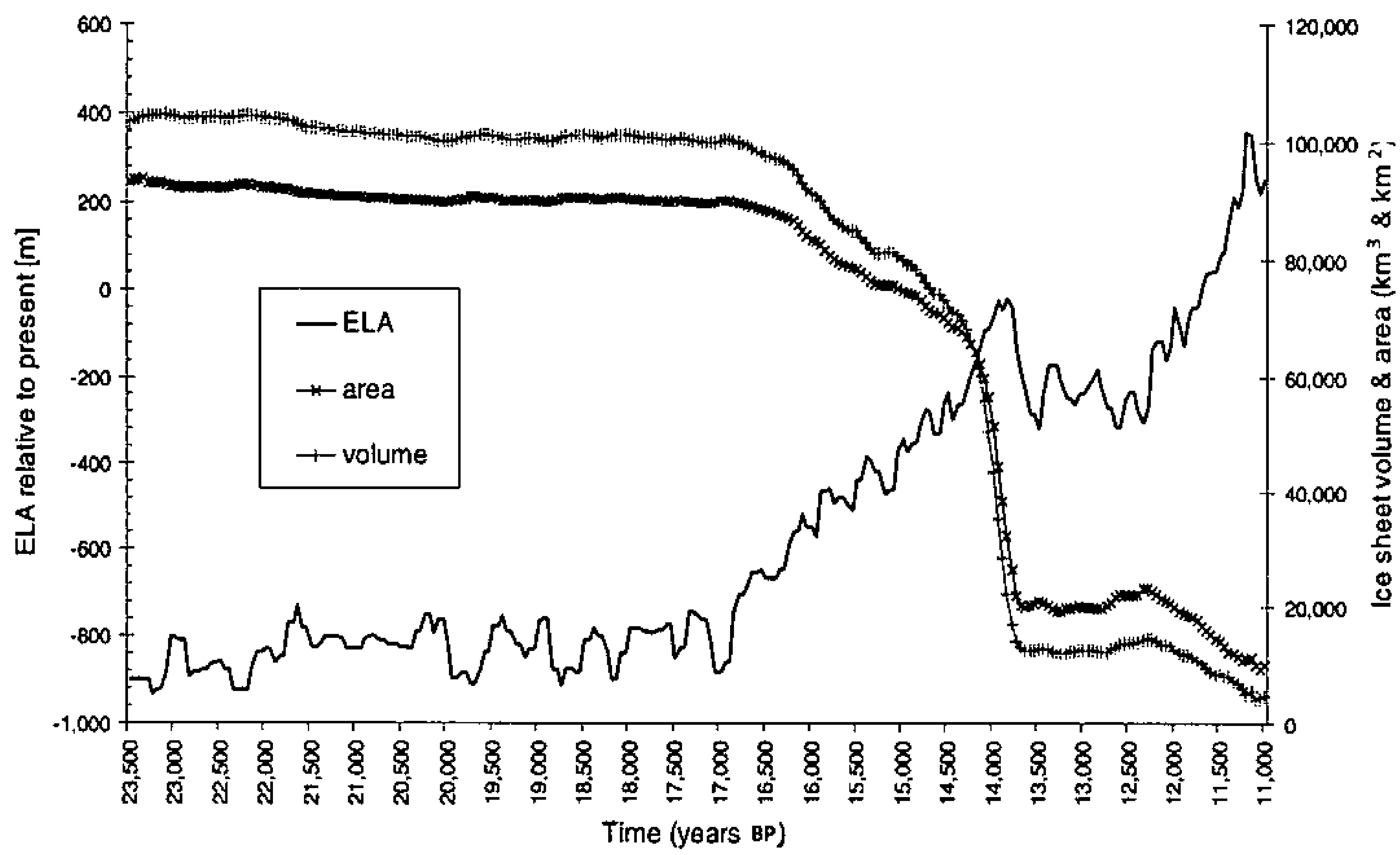

Fig. 7. Time-series of ice sheet volume and area during deglaciation from the optimum LGM extent at 23 500 through to 11 000 years BP driven by ELA re-scaled from the Vostok temperature reconstruction (Petit *et al.* 1999; see text)

undergoes catastrophic collapse, first in its western, seaward sector around 14 000 a BP (Fig. 8d) and then across the entire ice sheet, which by 13 500 a BP, is a mere shadow of its former self (Fig. 8e). During this collapse, the volume of the ice sheet falls from 70 000 to just over 10 000 km^3 in less than 800 years (Fig. 7), whilst in the same period, its area declines by *c.* 80%. At 13 800 a BP, this greatly reduced ice sheet, not significantly larger than the present-day NPI in terms of ice volume but with eastern and western outlet glaciers extended into lowland troughs, stabilizes and advances somewhat over the next 1500 years, in phase with the Antarctic Cold Reversal. At the end of this cold phase (*c.* 12 300 years BP) with climatic amelioration, this residual ice sheet then undergoes steady shrinkage up to 11 500 a BP resulting in limits (Fig. 8f) which closely resemble the present-day extent of the NPI.

Discussion

Our suite of model experiments indicates that a regional ELA reduction of 750 to 950 m yields an LGM ice sheet which matches the Fenix I to V moraine sequence at LBA. Within this broad range, an optimum model experiment was achieved with 900 m of ELA lowering which best fitted the Fenix V limit at 23 000 a BP (Kaplan *et al.* 2004) and Caldenius' (1932) regional LGM limit (Fig. 4). However, prudence is certainly advised before overly interpreting the palaeoclimatic significance of this result since sensitivity experiments revealed the modelled ice sheet to be rather dependent on the mass-balance parameters used. The OLE represents one of potentially many model scenarios that could produce a simulation matching the empirical evidence and hence should be considered no more than indicative. Despite this, it is worth noting that the regional ELA depression is certainly in good correspondence with general LGM palaeotemperature estimates in the mid-latitudes of South America (Broecker and Denton 1989), and the palaeoecological record from 40°S which indicated a temperature decrease of 6–7°C (Denton *et al.* 1999; Moreno *et al.* 1999). Although simplistic, given an assumed mean lapse rate of *c.* 0.0075°C m^{-1}, which is within bounds accepted by Kerr and Sugden (1994), then our modelled 900 m of LGM ELA lowering is realistic.

The optimum LGM ice sheet has a low aspect ratio breached by numerous large mountain massifs (e.g. Cerro San Lonenzo, Arnales, Pared Norte and San Valentin) and a number of smaller nunataks

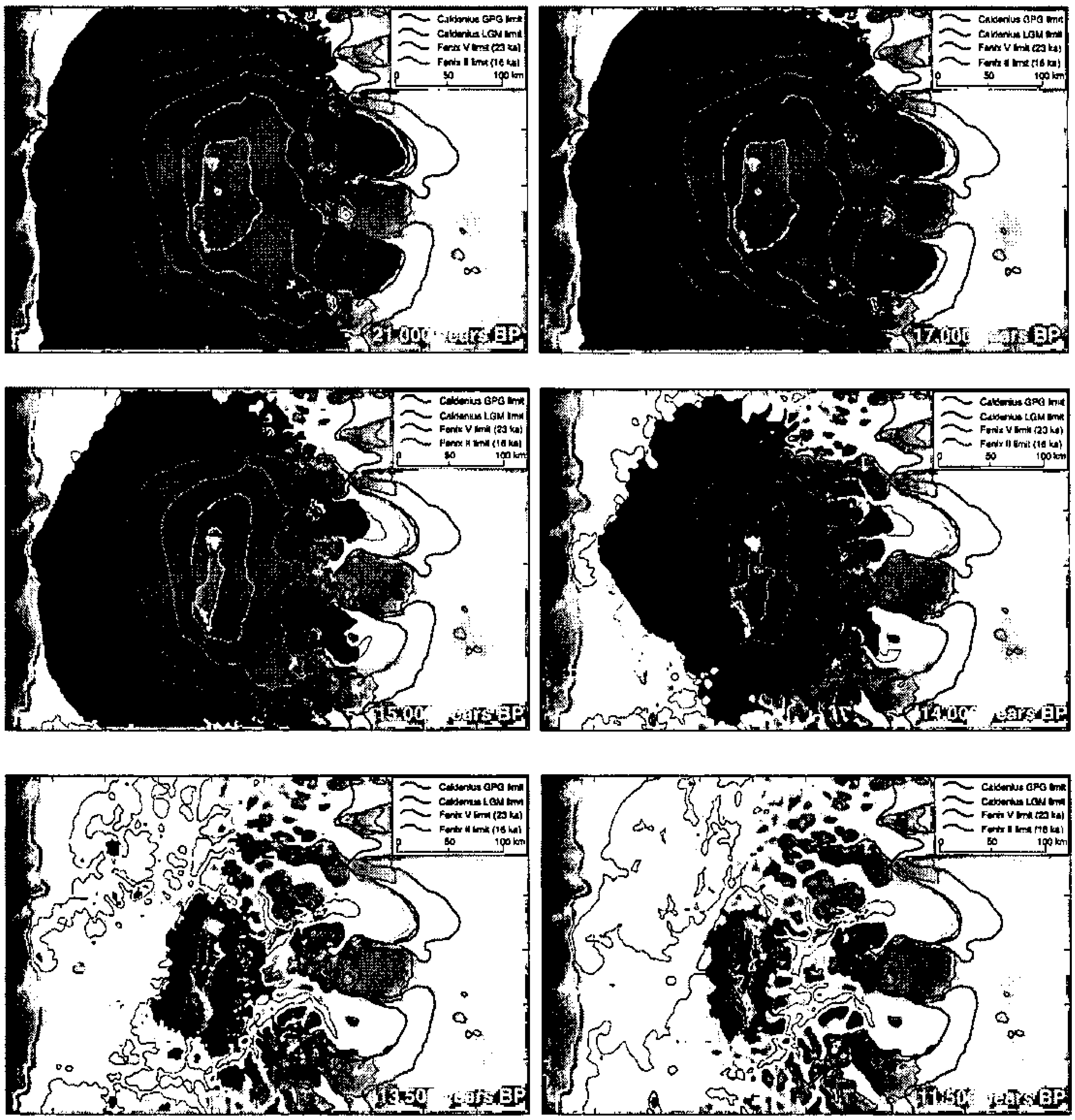

Fig. 8a–f. Time-slices of ice sheet surface elevation and isostatic adjustment at key snap-shots during deglaciation

(Fig. 9). With a total volume of just 103 247 km^3 distributed over an area of 91 872 km^2 yielding a mean ice thickness of *c.* 1130 m, this ice sheet certainly could be considered thin compared to the LGM reconstructions of Hulton *et al.* (1994, 2002). However, examination of the basal velocity pattern illustrates the key role that fast flow plays in effectively drawing down the main central ice-mass. The interior is penetrated and drained by a number of large, topographically controlled ice streams and outlet lobes which are fed by numerous tributaries and flow up to 2000 m a^{-1} (Fig. 10). Compared to the LGM model of Hulton *et al.* (1994, 2002), of critical importance are the two fast-flowing outlet lobes occupying LBA and Lago Pueyrredon (a.k.a. Cochrane) which effectively drain the ice sheet interior and prevent excessive ice build-up and runaway eastward expansion of the ice sheet with concomitant ice divide migration. The Lago Pueyrredon and LBA outlet lobes are characterized by low surface gradients (*c.* 1:20) and low basal shear traction (0.3–0.6 bar) associated with basal sliding and

Fig. 9. Rendered three-dimensional view of the optimum LGM model experiment from the Northeast illustrating the major mountains which penetrate the ice sheet along with numerous smaller nunataks and the large, fast-flowing outlet lobes that occupy Lagos Buenos Aires and Cochrane

Fig. 10. Modelled ice sheet surface velocity (m a−1) for the optimum LGM experiment showing extensive zones of ice-streaming to the west and north marine margins and the two fast-flowing outlet lobes occupying Lagos Buenos Aires and Cockrane to the east

ice-streaming behaviour. These results are in agreement with the work of Douglass *et al.* (2002) who used the direction of streamlined landforms and moraine long-profiles to reconstruct the outlet glacier occupying LBA, which was characterized by low surface gradients and basal shear stresses. Furthermore, geomorphic evidence for extensive basal sliding is found in various guises. Bedrock striations and other subglacially formed ice flow indicators have been observed around the lake and on

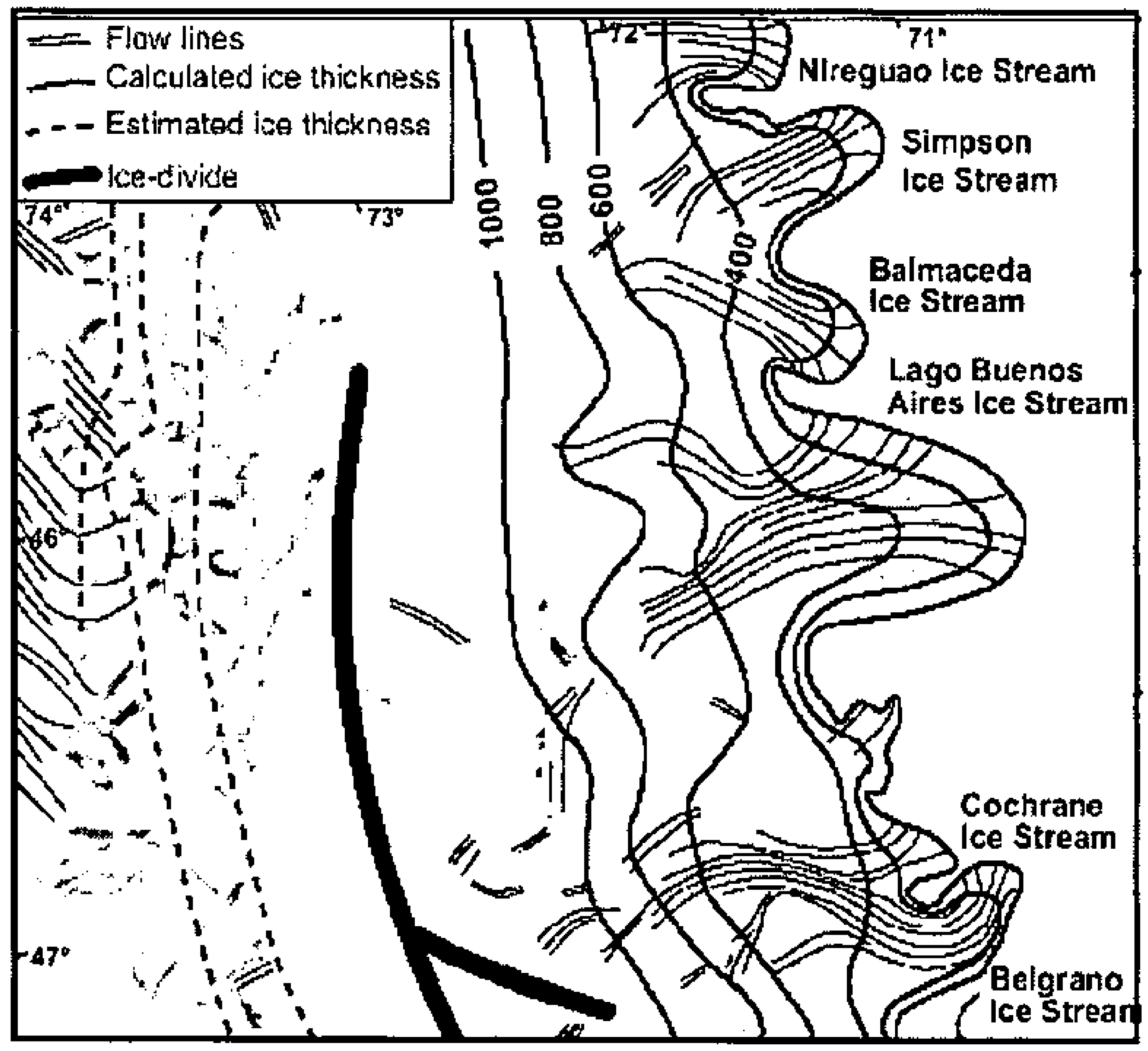

Fig. 11. Reconstruction of the fast-flowing outlet glaciers that drained the eastern portion of the NPI at the last glacial maximum. The reconstruction is based on mapped landforms (glacial lineations) and shows flowlines (defined by flowsets) and ice surface topography of the NPI at the LGM (adapted from Glasser and Jansson, 2005)

its islands (Douglass *et al.* 2002; Glasser and Jansson 2005; Glasser *et al.* 2004). Glasser and Jansson's (2005) semi-quantitative reconstruction based on Landsat imagery and geomorphological evidence corroborates that the LGM icecap was drained by a number of fast-flowing outlet glaciers characterized by a narrow main trunk with sharp lateral boundaries, parallel conformity between individual glacial lineations, convergent head areas and attenuated glacial lineations (summarized in Fig. 11). Furthermore, the large basaltic erratics on Fenix II are glacial polished and have striations (Singer *et al.* 2004), and the Fenix glacial events led to extensive glacio-fluvial outwash systems with well developed meltwater channels preserved to the present (see Fig. 2 in Singer *et al.* 2004). Although much of the melt could have come from the margin and top surfaces, roadcuts show that these moraines consist of reworked outwash and flow tills. These lines of evidence taken together confirm warm-based ice at least at the valley bottom, with extensive sub-glacial water and concomitant sliding at the bed.

Use of the 'independent' Vostok palaeotemperature reconstruction, which includes the 'classic' **Antarctic Cold Reversal (ACR)** from *c.* 14 500 to 12 800 a BP, produces good agreement with the sequence of events as defined by Kaplan *et al.* (2004) and Turner *et al.* (2005) for the LBA (Argentina) and Lago General Carrera (Chile) valleys. Steady overall retreat of the ice margin from Fenix V to I is dictated by the modest warming after the regional and global glacial maximum, *sensu stricto*, prior to *c.* 23 000 a BP. A number of small ELA oscillations (of *c.* 100 m amplitude) from 23 000 to 17 000 a BP result in a series of minor fluctuations in the margins of eastern outlet lobes which are consistent with the millennial scale deposition of the moraines, and which culminates in a readvance to the Fenix II position at 17 000 a BP. Subsequently, gradual warming in the temperature record drives a slow but steady retreat from 17 000 to 14 500 a BP, which agrees with the sequence of glacial events across LBA and Lago General Carrera. Sometime between 16 000 and 14 000 a BP, the dated geologic record indicates an abrupt and pronounced deglaciation (Turner *et al.* 2005); the modelled loss of ice once again mirrors the evidence, when driven by the Vostok record. Fenix I formed at *c.* 16 000 a BP, which was followed by a lake and readvance of the undated Menucos moraine (Kaplan *et al.* 2004). The record of Turner *et al.* (2005) then indicates that by 13 600 a BP ice stabilized or advanced and blocked drainage to the Pacific Ocean, forming a glacial lake. Finally, the modelled event shows broad agreement with the timing of an ACR-type event as outlined by Turner *et al.* (2005). The similarity between the terrestrial record and modelled sequence of events, when driven by the Vostok temperature curve, lends support to the idea that the Antarctic/Southern Ocean Climate and middle latitude South America are at least broadly linked during deglaciation.

Conclusions

Given an understanding of the past glacio-climatic regimes, we hope that this study demonstrates that high resolution modelling reliably captures the configuration and dynamics of the LGM ice sheet as represented in the geomorphologic record.

The western, seaward margin of the NPI is susceptible to widespread glaciation with an ELA lowering of just 400 m resulting in extensive ice sheet advance to the Pacific shelf. Due to the significant climatic gradient which exists across the Andes, significantly greater ELA depression of 750 to 950 m is required to advance ice to the eastern LGM limits as indicated by the Fenix I to V suite of moraines.

A region-wide ELA lowering of 900 m yields an optimum fit with Caldenius' (1932) LGM reconstruction and the Fenix V moraine which was deposited at *c.* 23 000 yr BP. This optimum LGM experiment resulted in a low aspect ice sheet with a volume of 103 247 km^3 distributed over an area of 91 872 km^2 which was efficiently drained and drawn down by numerous ice-streams, extending to the continental shelf in the west and with two large, fast-flowing outlet lobes to the east.

Driving the model from the LGM to the Holocene using a rescaled Vostok record results in a complex deglaciation sequence which is in good agreement with empirical reconstructions and supports the hypothesized climatic links between the Antarctic/Southern Ocean and mid-latitude South America.

After re-advancing to the Fenix II moraine at 17 000 a BP, the ice sheet slowly wanes with steady climatic amelioration until 14 500, a BP after which it rapidly collapses by 85% to a size not much larger than the present-day NPI within *c.* 800 years. After this it stabilizes for *c.* 1 500 years corresponding to the Antarctic Cold Reversal, before retreating to its present-day configuration by 11 000 a BP.

Acknowledgements

The authors would like to thank Brad Singer, Dan Douglas, David Sugden and anonymous reviewers for contributions and insightful comments from which this work has benefited greatly. We also appreciate the support of Steve Dowers and the computing staff at Edinburgh School of Geography and gratefully acknowledge financial support from the Royal Geographical Society (Michael Palin's Gumby Co.), the Royal Society and the Royal Society of Edinburgh.

Alun Hubbard, School of GeoSciences, Drummond Street, University of Edinburgh, Edinburgh, EH 9XP, Scotland, UK
E-mail: alh@geo.ed.ac.uk

Andrew S. Hein, School of GeoSciences, Drummond Street, University of Edinburgh, Edinburgh, EH 9XP, Scotland, UK
E-mail: ahein98@hotmail.com

Michael R. Kaplan, School of GeoSciences, Drummond Street, University of Edinburgh, Edinburgh, EH 9XP, Scotland, UK
E-mail: mike.kaplan@ed.ac.uk

Nick R.J. Hulton School of GeoSciences, Drummond Street, University of Edinburgh, Edinburgh, EH 9XP, Scotland, UK
E-mail: nyh@geo.ed.ac.uk

Neil Glasser, Centre for Glaciology, Institute of Geography and Earth Sciences, University of Wales, Aberystwyth, Ceredigion SY23 3DB, Wales UK
E-mail: nfg@aber.ac.uk

References

Becquey, S. and Gersonde, R., 2003: A 0.55-Ma paleotemperature record from the Subantarctic zone: Implications for Antarctic Circumpolar Current development. *Paleooceanography*, 18(1): DOI 10.1029/2000PA000576.

Boulton, G.S., Hagdorn, K.M. and Hulton, N.R.J., 2003: Streaming flow in an ice sheet through a glacial cycle. *Annals of Glaciology*, 36: 117–128.

Broecker, W. S. and Denton, G. H., 1989, The role of ocean-atmosphere reorganizations in glacial cycles. *Geochimica et Cosmochimica Acta*, 53: 2465–2501.

Caldenius, C. G., 1932: Las glaciaciones Cuaternarias en la Patagonia and Tierra del Fuego. *Geografiska Annaler*, 14: 1–164.

Casassa, G. 1987: Ice thickness deduced from gravity anomalies on Soler Glacier, Nef Glacier and NPI. *Bulletin of Glacier Research*, 4.

Casassa, G., Rivera, A., Aniya, M. and Naruse R., 2002: Current knowledge of the Southern Patagonia Icefield. *In*: Casassa, G.

Sepúlveda, F. and Sinclair, R. (eds): The Patagonian Icefields. A unique natural laboratory for environmental and climate change studies. Kluwer Academic/Plenum Publishers. New York. 67–83.

Denton, G.H., Heusser, C.J., Lowell, T.V., Moreno, P.I., Andersen, B.G., Heusser, L.E., Schluchter, C. and Marchant, D.R., 1999: Interhemispheric linkage of paleoclimate during the last glaciation. *Geografiska Annaler*, 81: 107–153.

Douglass, D.D., Kaplan, M.R., Singer, B.S. and Mickelson, D.M., 2002: A low gradient outlet glacier of the Patagonian ice cap at Lago Buenos Aires, Argentina, during the last glacial maximum. Geological Society of America Annual meeting Programs with Abstracts.

EPICA, 2004: Eight glacial cycles from an Antarctic ice core, *Nature*, 429: 623–628.

Fairbanks, R.G., 1989: A 17 000-year glacio-eustatic sea level record; influence of glacial melting rates on the Younger Dryas event and deep-ocean circulation. *Nature*, 342(6250): 637–642.

Glasser, N.F. and Jansson, K. 2005: Fast-flowing outlet glaciers of the last glacial maximum Patagonian Icefield. *Quaternary Research*, 63(2): 206–211.

Hagdorn, K.M., 2003: Reconstruction of the Past and Forecast of the Future European and British Ice Sheets and Associated Sea–Level Change. Ph.D. thesis, University of Edinburgh.

Hindmarsh, R., 1993: Modelling the dynamics of ice sheets. *Progress in Physical Geography*, 17(4): 291–313.

Holling, J.T. and Schilling, D.H., 1981: Late Wisconsin-Weichselian Mountain Glaciers and Small Ice Caps. *In*: Denton, G.H. and Hughes, T.J. (eds): The Last Great Ice Sheets. John Wiley & Sons. New York. 179–206.

Hubbard, A. 1997: Modelling climate, topography and palaeoglacier fluctuations in the Chilean Andes. *Earth Surface Processes and Landforms*, 22: 79 –92.

Hubbard, A. 1999: High resolution modelling of the advance of the Younger Dryas Ice Sheet and its climate in Scotland. *Quaternary Research*, 52: 27–43.

Hubbard, A. et al. (in press): A modelling insight into the Icelandic Late Glacial Maximum ice sheet. *Quaternary Science Review*.

Hulton, N.R.J. and Sugden, D.E. 1997: Dynamics of Mountain ice caps during glacial cycles: The case of Patagonia. *Annals of Glaciology*, 24: 81–89.

Hulton, N. Sugden, D.E., Payne, A.J. and Clapperton, C.M. 1994: Glacier modelling and the climate of Patagonia during the Last Glacial Maximum. *Quaternary Research*, 42: 1–19.

Hulton, N.R.J., Purves, R.S., McCulloch, R.D., Sugden, D.E. and Bentley, M.J. 2002: The last glacial maximum and deglaciation in southern South America. *Quaternary Science Reviews*, 21: 233–241.

Kaplan, M.R., Ackert, R.P., Singer, B. S., Douglass, D.C. and Kurz, M.D., 2004. Cosmogenic nuclide chronology of millennial-scale glacial advances during O-isotope Stage 2 in Patagonia. Geological Society of America Bulletin 116, 308–321.

Kaplan, M.R., Douglass, D.C., Singer, B.S., Ackert, R.P. and Caffee, M.W. 2005: Cosmogenic nuclide chronology of pre-last glaciation maximum moraines at Lago Buenos Aires, 46°S, Argentina. *Quaternary Research*, 63: 301–315.

Kerr, A.R. and Sugden, D.E. 1994: The sensitivity of the South Chilean snowline to climatic change, *Climatic Change*, 28: 255–272

Lamy, F., Kaiser, J., Ninnemann, U., Hebbeln, D., Arz, H.W. and Stoner J., 2004: Antarctic timing of surface water changes off Chile and Patagonian Ice Sheet response. *Science*, 304: 1959–1962.

Lliboutry L., 1998: Satellite image atlas of glaciers of the world. Geological Survey Professional Paper. Glaciers of South America, Series. Washington. 206 p.

Marshall, S.J. and Clarke, G.K.C., 1999: Ice sheet inception: subgrid hypsometric parameterization of mass balance in an ice sheet model. *Climate Dynamics*, 15: 533–550.

Mercer, J.H., 1983: Cenozoic glaciation in the southern hemisphere. *Annual Reviews of Earth and Planetary Science*, 11: 99–132.

McCulloch, R.D., Bentley, M.J., Purves, R.S., Sugden, D.E., Hulton, N.R.J. and Clapperton, C., 2000: Climatic inferences from glacial and palaeoecological evidence at the last glacial termination, southern South America. *Journal of Quaternary Science*, 15: 409–417.

Moreno, P. I., Jacobson, G. L., Andersen, B. G., Lowell, T. V. and Denton, G. H. 1999: Vegetation and climate changes during the last glacial maximum and the last termination in the Chilean Lake District: A case study from Canal de la Puntilla (41°S). *Geografiska Annaler*, 81A: 285–311.

Murdie, R.E., Pugh D. T. and Styles, P., 1999: A lightweight, portable, digital probe for measuring the thermal gradient in shallow water sediments, with examples from Patagonia. *Geo-Marine Letters*, 18: 315–320.

Paterson, W.S.B., 1994: Physics of Glaciers (3rd edn), Pergamon Press. New York. 480 p.

Petit J.R., Jouzel J., Raynaud D., Barkov N.I., Barnola J.M., Basile I., Bender M., Chappellaz J., Davis J., Delaygue G., Delmotte M., Kotlyakov V.M., Legrand M., Lipenkov V., Lorius C., Pépin L., Ritz C., Saltzman E. and Stievenard M., 1999: Climate and atmospheric history of the past 420 000 years from the Vostok Ice Core, Antarctica. *Nature*, 399: 429–436.

Porter, S. C. 1981: Pleistocene glaciation in the southern Lake District of Chile. *Quaternary Research*, 16: 263–292.

Prohaska, F., 1976: The climate of Argentina, Paraguay, and Uruguay: *In*: Schwerdtfeger, W., (ed.): Climates of Central and South America. World Survey of Climatology, vol. 12. Elsevier, New York, 13–112.

Rabassa, J. and Clapperton, C. M., 1990: Quaternary glaciations in the southern Andes: *Quaternary Science Reviews*, 9: 153–174.

Rignot, E., Rivera, A. and Casassa, G., 2003: Contribution of the Patagonia Icefields of South America to Global Sea Level Rise, *Science*, 302: 434–437.

Singer, B.S., Ackert, R.P. and Guillou, H., 2004: $^{40}Ar/^{39}Ar$ and K-Ar chronology of Pleistocene glaciations in Patagonia. *Geological Society of America Bulletin*, 116: 434–450.

Turner, K.J., Fogwell, C.J., McCulloch, R.D. and Sugden, D.E. 2005: Deglaciation of the eastern flank of the NPI and associated continental-scale lake diversions. *Geografiska Annaler*, 87A(2): 363–374.

Van der Veen, C.J., 1999: Fundamentals of Glacier Dynamics. A.A. Balkema. Rotterdam.

Vimeux, F., Cuffey, K.M. and Jouzel,J., 2002: New insights into Southern Hemisphere temperature changes from Vostok ice cores using deuterium excess correction, *Earth and Planetary Science Letter*, 203: 829–843.

Wenzens, G. 2003: Comment on: 'The Last Glacial Maximum and deglaciation in southern South America' - by N.R.J. Hulton, R.S. Purves, R.D. McCulloch, D.E. Sugden, M.J. Bentley [*Quaternary Science Reviews*, 21(2002) 233–241]. *Quaternary Science Reviews*, 22(5): 751–754.

Manuscript received November 2004, revised and accepted January 2005.